Chapter 5

Electrodeposition of Cu–Ni Composite Coatings

Casey R. Thurber, Adel M.A. Mohamed and Teresa D. Golden

Additional information is available at the end of the chapter

http://dx.doi.org/10.5772/62111

Abstract

The electrodeposition of Cu–Ni incorporated with nano- to microparticles to produce metal matrix composites has been reviewed in this chapter. The inclusion of particles into the metal matrix produced enhanced properties in the areas of electronics, mechanics, electrochemistry, and corrosion. In electronics, an increase in the magnetic properties and durability for microactuators was observed. Measurements of the mechanical properties showed an increase in hardness, wear resistance, shear adhesion, and tensile strength for the material. The corrosion resistance of the metal matrix coatings was improved over that of pure Cu–Ni. As the accessibility of nanoparticles continues to increase, the interest in reduced cost and low-temperature electrodeposited metal matrix composites continues to rise. However, only a small number of articles have investigated Cu–Ni composite coatings; these composite coatings need further examination due to their advantageous properties.

Keywords: Electrodeposition, Metal Matrix Composites, Cu-Ni alloys, Coatings, Nanoparticles

1. Introduction

Metal matrix composite (MMC) coatings engineered using an electrodeposition method are examined in this chapter. The electrodeposition of a composite involves the electrolysis of plating baths where nano- to micro- sized particles are dispersed and various quantities of the particles become imbedded within the plated metal matrix, providing special properties to the coating (Figure 1) [1]. The process of particle incorporation into metal coatings can be simplified into four steps: (1) particles dispersed in solution form a surface charge; (2) from the bulk solution, there is mass transport of the particles to the surface of the electrode typically through convection; (3) there is interaction between the particle and the electrode; (4) the particles become trapped within the growing metallic film [2]. The earliest example of electrodeposited

INTECH
open science | open minds

© 2016 The Author(s). Licensee InTech. This chapter is distributed under the terms of the Creative Commons Attribution License (http://creativecommons.org/licenses/by/3.0), which permits unrestricted use, distribution, and reproduction in any medium, provided the original work is properly cited.

composites dates back to the 1920s where Cu–graphite coatings were developed for automotive bearings [3, 4]. Enhanced corrosion, tribological, and mechanical properties were the main research focus of the automotive and aerospace industries in the 1970s–1990s, leading to significant technological advancements. In the early 2000s, some of the focus started to shift to electrical components and electronic devices [5–10]. As the accessibility of nanoparticles continues to rise, the interest in reduced cost and low-temperature electrodeposited MMCs continues to escalate [2].

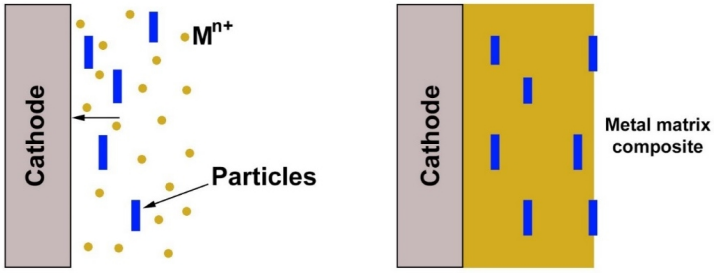


Figure 1. Schematic displaying the growth of MMCs by electrodeposition.

Coatings can be produced by using several different approaches, and electrodeposition remains a prominent technique to produce novel materials for science and engineering applications. Electrodeposition also offers low cost, convenience, ability to work at low temperatures, and the ease of application to complex geometries [11, 12]. Other advantages for using electrodeposition include the ability to quickly scale to an industrial setting, uniform coating of large samples, and accurate control of the coating thickness [2]. Other methods for producing MMCs include commercial pressing [13], laser cladding [14], hot pressing [15], plasma transferred-arc surfacing [16], stir casting [17], diffusion bonding [18], powder metallurgy [19], and chemical vapor deposition [20]. Each of these methods has different advantages and disadvantages. However, some of the drawbacks include production at high temperatures or under vacuum, difficulty in controlling the thickness, and cost.

MMCs coatings combine the advantageous properties of each individual material together which is not possible with the non-composite metal films [21, 22]. An extensive amount of work has gone into examining copper-based MMCs [23–27] and nickel-based MMCs [28–32] since individual metals can exhibit a limited range of properties. An important route to improving the properties of individual metals is the deposition of alloys such as Zn–Ni, Ni–Mo, and Cu–Ni [33–35]. Successful incorporation of particles into the metal matrix by electrocodeposition relies on many different parameters, including the composition of the electrolyte, pH, current density, and properties of the particles [36]. Incorporating particles such as TiO_2, SiC, Al_2O_3, carbon fibers, Ni, Al, and Cr into the Cu–Ni matrix of different coatings enhances the electrical, mechanical, and corrosion properties of the coatings [5–9, 21, 37–40].

Copper alloys, such as Cu–Ni, have been studied because of their good electrical and thermal properties, machinability, and resistance to corrosion [41–44]. Copper is relatively soft and

http://dx.doi.org/10.5772/62111

needs to be alloyed with another metal, such as nickel, to increase the hardness of the material [43, 45]. Also, with the addition of Ni into the Cu matrix during electrodeposition, it is possible to grow films with minimal strain due to both Cu and Ni having face-centered cubic crystal structures and similar lattice parameters [46]. The electroplating of copper alloy films has an instrumental role in many different industry-related applications. For instance, electroplating has found a niche in microelectromechanical systems (MEMS) because the process can deposit different alloys onto depressed and oddly shaped geometric substrates [5, 6, 10, 45]. Cu–Ni coatings have been evaluated for use as inert anodes in the fabrication of aluminum because of their enhanced electrical and thermal conductivity [8, 9]. In marine environments, copper alloys are used to defend against biofouling of materials by inhibiting microbial-induced corrosion (MIC) [47–50].

Understanding the incorporation of particles into these alloys requires mathematical modeling. Early models dating back to the 1960s from Williams and Martin [51] proposed that particles were transported to the cathode surface via a convection transport mechanism facilitated by stirring the plating bath. Brandes and Goldthorpe [52] hypothesized that entrapment by mechanical means was not the only factor at play and decided that an electrostatic force must be aiding the inclusion of the particles into the metal matrix. In 1972, Guglielmi [53] became the first to propose a mathematical model that explained the inclusion of particles into the metal matrix. The model followed a simple two part approach: (a) the particles slowly move toward the surface of the cathode and adsorb very loosely and (b) then the particles become securely adsorbed by shedding their ionic cloud. The derived model equations are [40, 53]:

$$\frac{C\left(1-\alpha\right)}{\alpha}=\frac{Wi_o}{nFd\upsilon_o}e^{(A-B)\eta}\left(\frac{1}{k}+C\right) \tag{1}$$

$$i=\left(1-\vartheta\right)i_o e^{A\eta} \tag{2}$$

where C is the vol.% of particles in the electrolyte solution and α is the vol.% of the particle incorporated in the composite film. W corresponds to the atomic weight of the metal in the coating, F is Faraday's constant, d is the density of the metallic coating, and n is the valence of the metallic coating. η relates to the overpotential, i is the current density, and i_o is the current density from the metallic coating. The υ term is a constant from the deposition of the particle, A is a constant from the deposition of the metal, and B is a constant from the particle inclusion. The ϑ relates to the coverage of the surface by the particle that is incorporated into the metal coating and k is the adsorption coefficient. Although the model has some holes, such as not taking into account the mass transport of the metal ions or the particles and the nature of the particle or the shape, it is still one of the most widely used models to date. In 1987, Celis et al. [54] hypothesized a nnew five part model, which is built on the idea of Guglielmi's two part model. The drawback of this model is that factors need to be created that are specific to each individual system. As late as 2002, Bercot's group [55] proposed an addition to Guglielmi's original model that included a polynomial for the purpose of correcting for different effects presented by adsorption and flow.

A survey of the literature for the incorporation of particles into Cu–Ni coatings is shown in Table 1. The composite coatings described in Table 1 are for electrodeposited processing only. Other Cu–Ni composites have been made using different techniques, but fall outside the scope of this chapter.

This chapter will cover the electrodeposition of Cu–Ni alloys onto steels and other substrates to improve corrosion resistance and mechanical properties. The influence of the deposition parameters will be covered as well as the electrodeposition mechanism. The resulting mechanical and corrosion properties will also be discussed in the chapter.

Reference	Possible Applications	Deposition Conditions	Composite
Panda et al. [5]	Recessed microelectrodes for MEMS devices	1.0 M $NiSO_4 \cdot 6H_2O$ 0.04 M $CuSO_4 \cdot 5H_2O$ 0.3M $Na_3C_6H_5O_7 \cdot 2H_2O$ 3.125–12.5 g/L Al_2O_3 j = 2–50 mA/cm^2 26°C	Cu–Ni alloy incorporated with γAl_2O_3 (~30 nm)
Huang et al. [10]	Magnetic microactuators for MEMS Devices	200–250 g/L $CuSO_4 \cdot 5H_2O$ 45–90 g/L H_2SO_4 Plating rate: ~0.2 μm/min 40°C	Cu incorporated with Ni nanopowder (~50 nm)
Chen et al. [6]	Electrical and electronics (speakers)	Alkaline noncyanide-based copper-plating solution 2–8.5 g/L Ni 40°C Stir rate: 250 rpm	Cu incorporated with Ni nanoparticles
Huang et al. [8, 9]	Electrical and electronics (MEMS devices)	120 g/L $Na_3C_6H_5O_7 \cdot 2H_2O$ 25 g/L H_3BO_3 12 g/L $NiCl \cdot 7H_2O$ 100 g/L $NiSO_4 \cdot 7H_2O$ 5–25 g/L $CuSO_4 \cdot 5H_2O$ j = 0.5–2 A/cm^2 35°C	Cu–Ni incorporated with Cr nanoparticles (~40 nm)
Chrobak et al. [21]	Mechanical and Young's modulus	150 g/L $CuSO_4 \cdot 5H_2O$ 10 g/L H_2SO_4 Ni 0.1–20 mg/mL j = 1–100 mA/cm^2	Cu incorporated with Ni nanoparticles (~100 nm)
Fawzy et al. [37]	Mechanical and hardness	50 g/dm^3 $Na_3C_6H_5O_7 \cdot 2H_2O$ 25 g/dm^3 H_3BO_3 50 g/dm^3 $Na_2SO_4 \cdot 10H_2O$ 40 g/dm^3 $NiSO_4 \cdot 7H_2O$ 5–25 g/dm^3 $CuSO_4 \cdot 5H_2O$ j = 0.33–1.33 A/dm^2 0–20 g/dm^3 Al_2O_3 and TiO_2	Cu–Ni incorporated with Al_2O_3 and TiO_2

Reference	Possible Applications	Deposition Conditions	Composite
Hashemi et al. [38]	Mechanical, hardness, and wear	90 g/L $H_3C_6H_5O_7$ 60 g/L NaOH 60 g/L $Na_2WO_4 \cdot 2H_2O$ 20 g/L $NiSO_4 \cdot 7H_2O$ 1 g/L $CuSO_4 \cdot 5H_2O$ 0–25 g/L SiC j = 10–50 mA/cm^2 Stir rate = 100–600 rpm	Cu–Ni–W incorporated with SiC (~50 nm)
Wan et al. [39]	Mechanical and tensile strength	*Bath Conditions Not Given	Cu–Ni reinforced carbon fibers (6–8 μm)
Cui et al. [40]	Electrochemical Study for Magnetic and mechanical properties	184 g/dm^3 $NiSO_4 \cdot 6H_2O$ 6.24 g/dm^3 $CuSO_4 \cdot 5H_2O$ 76.47 g/dm^3 $Na_3C_6H_5O_7 \cdot 2H_2O$ 0.2 g/dm^3 Sodium dodecyl sulfate 0.5 g/dm^{3}saccharin Stir rate = 200 rpm j = 10-20 mA/cm^2 30°C	Cu–Ni incorporated with Al nanoparticles (3 μm)
Thurber et al. [60]	Mechanical, hardness, shear and corrosion	0.24 M $Ni(NH_4)_2(SO_4)_2 \cdot 6H_2O$ 0.06 M $CuSO_4 \cdot 5H_2O$ 0.25 M $Na_3C_6H_5O_7 \cdot 2H_2O$ MMT 0–0.2% E_{app} = –1.0V 25°C	Cu–Ni incorporated with MMT platelets

Table 1. A summary of the work produced on electrodeposited Cu–Ni composite coatings.

2. Cu–Ni MMCs in MEMS and Electronics

Cu–Ni composites have shown to be beneficial in the area of MEMS devices, microactuators, and electronics. Al_2O_3, Ni nanoparticles, and Cr particles have been incorporated into the metal matrix to produce improved mechanical properties, magnetic properties, and chromia scale for oxidation resistance [5, 6, 8–10].

Panda et al. [5] evaluated the electrodeposition of graded Ni–Cu alloys and Ni–Cu–γAl_2O_3 composites into deeply depressed electrodes made using X-ray lithography for use in MEMS devices. The rotating cylinder experiment showed that the current efficiency was below 100% for the deposition over a diverse range of current densities. With the inclusion of 12.5 g/L of alumina at a rotation rate of 1,000 rpm, it was found that the current efficiency was drastically lowered by the incorporation of the nanoparticles below 20 mA/cm^2 but produced deposits with higher copper content which was preferred. At the greater current densities (30–50 mA/cm^2), the current efficiency was less effected but lead to coatings with higher nickel content.

The Cu weight ratio was studied at different heights on the micropost for pure Cu–Ni and Cu–Ni–Al_2O_3 at current densities of 10 and 15 mA/cm^2, seen in Figures 2 and 3, respectively. A rise in the concentration of Cu along the post was expected due to the reduction of boundary layer thickness because of the diffusion-controlled reaction mechanism of copper. The composite micropost showed a sharp increase in the Cu concentration starting at about a height of 300 μm with the incorporation of alumina, which suggests that the incorporated nanoparticles into the plating bath helped to improve the mass transport at the site of the recess.

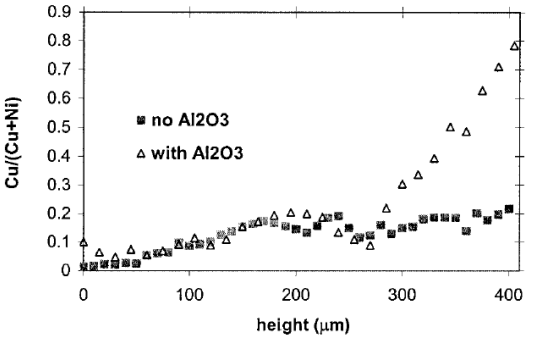


Figure 2. The copper weight ratio versus the height of the micropost with and without alumina for the current density of 10 mA/cm^2 and a duty cycle of 0.125. "Reproduced by permission of The Electrochemical Society." [5].

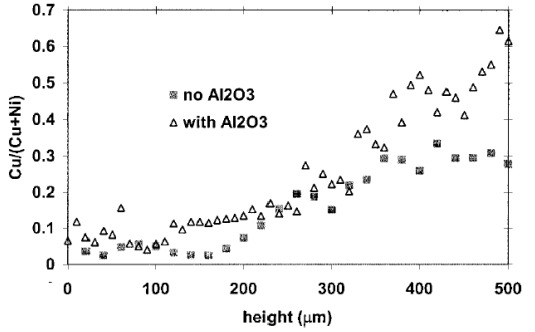


Figure 3. The copper weight ratio versus the height of the micropost with and without alumina for the current density of 15 mA/cm^2 and a duty cycle of 0.125. "Reproduced by permission of The Electrochemical Society." [5].

Huang et al. [10] experimented with a Cu–Ni composite from a plating bath consisting of an alkaline copper solution incorporated with 2–5 g/L of ~50 nm nickel nanoparticles to increase the performance in magnetic microactuators for MEMS. The superconducting quantum interference device (SQUID) measurements for magnetism seen in Figure 4 demonstrates that with the inclusion of ferromagnetic Ni particles into the copper matrix, the film shifts from

http://dx.doi.org/10.5772/62111

diamagnetic to ferromagnetic in nature as the curve becomes larger. The vertical displacement of the magnetic microactuator was measured for the actuator coils fabricated from copper and Cu–Ni composite materials. Figure 5 indicates that under the same experimental conditions, the Cu–Ni composite coil possessed a greater vertical displacement versus the pure Cu film, leading to about a 9% increase in the actuation enlargement performance.

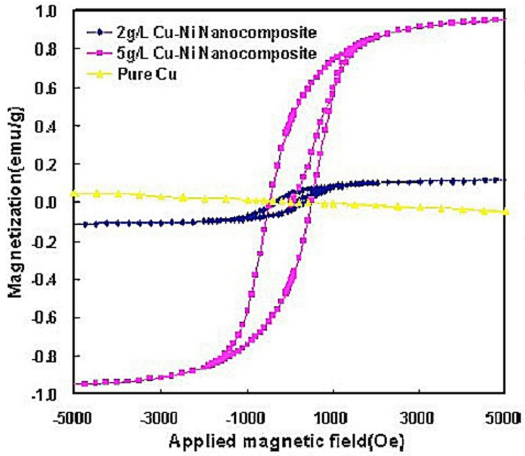


Figure 4. The SQUID measurements of copper versus the Cu–Ni composite electrodeposited from a bath that contained 2–5 g/L of nickel nanopowder. "Reprinted with permission from [10]. Copyright [2007], AIP Publishing LLC."

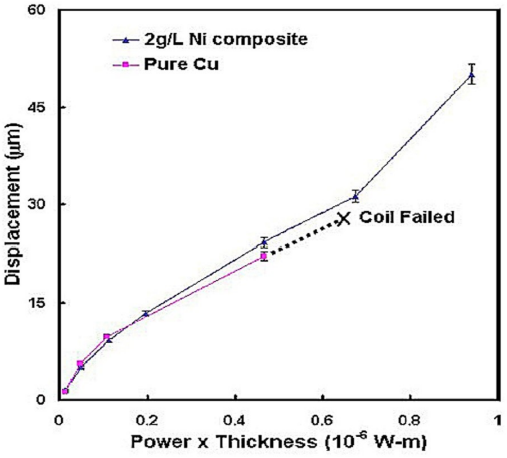


Figure 5. The vertical displacement results of the diaphragms compared to the normalized input experienced by the driving coils, which consists of the copper and Cu–Ni composite."Reprinted with permission from [10]. Copyright [2007], AIP Publishing LLC."

Chen et al. [6] proposed a new coil material for a reduced power electromagnetic microactuation device using Cu–Ni nanocomposites from an alkaline Cu-plating bath integrated with 2–8.5 g/L 100 nm nickel nanoparticles. Different coil widths ranging from 10–500 μm were examined with SQUID and resistivity measurements to determine the optimal power-saving microspeaker device. The SQUID and resistivity analysis found that the 200 μm wide inductive coil from the bath containing 2 g/L of Ni nanoparticles had optimal ferromagnetic characteristics with low resistivity. The sound pressure level was then evaluated for the pure copper and optimal Cu–Ni nanocomposite wire for a frequency ranging from 1–6 kHz, which resulted in a 40% power savings for the Cu–Ni nanocomposite versus the pure copper coil [6].

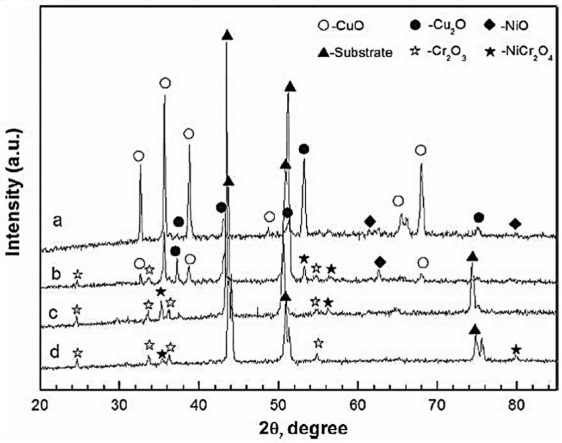


Figure 6. The stacked X-ray diffraction patterns of the Cr_2O_3 scale generated on four different samples after oxidation in atmosphere at 800 °C for 20 h: [a] commercial grade Cu–30Ni–20Cr, [b] commercial grade Cu–50Ni–20Cr, [c] electrodeposited Cu–30Ni–20Cr composite, and [d] electrodeposited Cu–50Ni–20Cr composite [9]."Reprinted with the permission of Cambridge University Press."

A crucial problem for extending the applications of Cu–Cr MMCs is poor resistance to oxidation, specifically in high-temperature environments for the electrical and electronic industries [8, 9]. This is due to the fact that at high temperatures chromium has a low solubility into copper, which greatly decreases the chromium amount diffusing to the surface of the copper matrix, preventing growth of the protective Cr_2O_3 scale. Nickel can be added into the matrix to increase the solubility of Cr into the composite to help increase the resistance to oxidation [9]. Huang et al. [8] discussed the electrodeposition of Cu–Ni–Cr, where copper and nickel were at a 1:1 ratio. They found that incorporating 15–20 wt.% Cr nanoparticles (~40 nm) into the Cu–Ni matrix allowed for a good chromia scale to form during the oxidation process in atmosphere at 800°C. It was found that incorporating less than 15 wt.% Cr lead to nonuniform growths of the chromia scale. Huang et al. [9] also examined the electrodeposition of Cu–30Ni–20Cr and Cu–50Ni–20Cr for the formationof the Cr_2O_3 protective scale. Figure 6 displays an X-ray diffraction pattern for the two electrodeposited coatings plus two commercially available alloys of the same composition after oxidation in atmosphere at 800°C. The

http://dx.doi.org/10.5772/62111

result shows that the commercial alloys mainly consist of more NiO, Cu_2O, and CuO after oxidation, whereas the electrochemically prepared coatings consist primarily of Cr_2O_3 and $NiCr_2O_4$. Figure 7 shows SEM pictures of the Cr_2O_3 scale created from the oxidation process at 800°C. It was discovered that for the electrodeposited samples the Cr_2O_3 scale quickly formed in the initial stage of growth and continued through the steady-state stage, where the coating acts as a reservoir for Cr to maintain the chromia scale growth. The commercially available sample Cu–50Ni–20Cr showed a similar result to the electrodeposited coatings but the Cu–30Ni–20Cr showed virtually no growth of the Cr_2O_3 scale, which showed that the commercial grade relied on an increase in Ni content to grow the chromia scale [9].

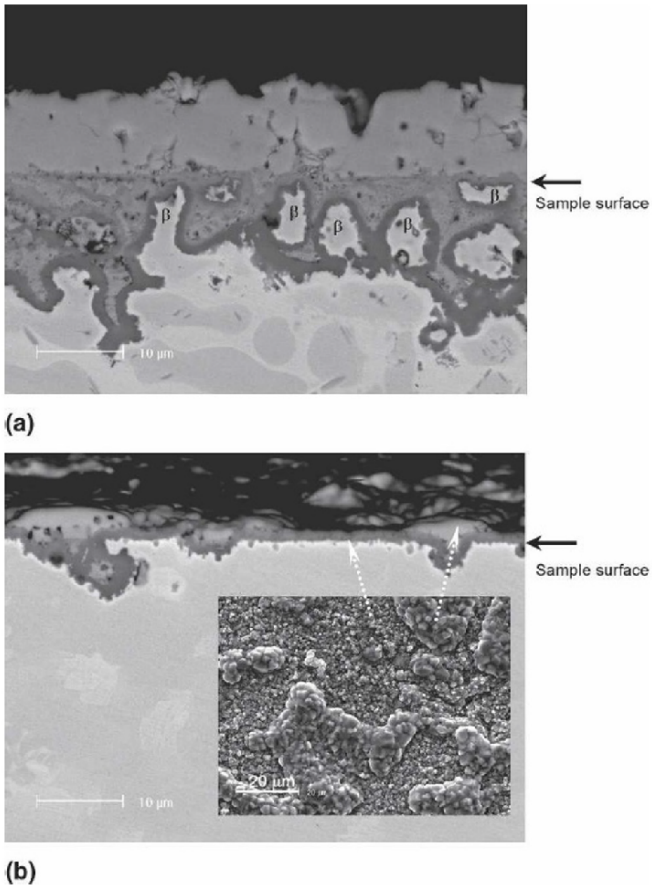


Figure 7. The cross-sectional SEM of the Cr_2O_3 scales formed on the surface of the Cu–Ni–Cr alloys of [a] Cu–30Ni–20Cr and [b] Cu–50Ni–20Cr, which was oxidized for 20 h in atmosphere at 800°C and the inset displays the structure of the different oxides at the surface, which are designated by arrows [9]."Reprinted with the permission of Cambridge University Press."

3. Cu–Ni MMCs for Enhanced Mechanical Properties

Particle incorporation can be used to improve mechanical properties for MMC coatings over that of the pure metal matrix. The Cu–Ni matrix has been incorporated with Ni particles, TiO_2, Al_2O_3, SiC, carbon fibers, and montmorillonite to increase the hardness, wear resistance, shear adhesion, and tensile strength [21, 37–39, 60].

Chrobak et al. [21] examined the electrodeposited copper incorporated with Ni powder (~100 nm) at varying current densities to examine the effects to Young's modulus. They experimented with current densities ranging from 1–100 $mAcm^{-2}$ and found that the concentration of Ni in the coating increases linearly with current density but the thickness of the coating decreases because the transport of Cu to the electrode surface is suppressed by the Ni particles. They also discovered that adding 25 vol.% of glycerol to the bath helped reduce agglomeration and decrease the grain size of the MMC coatings. The Young's modulus was found to decrease when the Ni concentration was increasing. This trend was even more drastic as the current density was increased because an increased current density leads to higher concentrations of Ni [21].

Fawzy et al. [37] examined how the current density, concentration of ceramic particles in the electroplating solution, and pH of the plating bath affected the hardness for Cu–Ni, Cu–Ni–αAl_2O_3, and Cu–Ni–TiO_2 composite coatings. By increasing the current density from 0.33 to 1.33 Adm^{-2} for the Cu–Ni–αAl_2O_3 and Cu–Ni–TiO_2 depositions, an increase in the Ni percentage in the coating and hardness was observed versus the pure Cu–Ni coating, but the percentage of the ceramic particles in the coating decreased. Increasing the pH of the plating solutions from 2.5 to 4.05 lead to an escalation in the Ni percentage in the film, loading percentage of the ceramic particles, and hardness. The hardness increased as the Al_2O_3 and TiO_2 increased in the plating solution from 170 to 248 kgf mm^{-2} for the addition of αAl_2O_3 particles with no effect to the Ni concentration in the coating, whereas the addition of TiO_2 particles produced an increase from 170 to 231 kgf mm^{-2} and helped to increase the Ni percentage in the coating. The optimal coating parameters were determined to be 1.33 A dm^{-2} for the current density, at pH 4.05, and incorporating 20 g dm^{-3} of the ceramic particles into the plating bath [37].

Hashemi et al. [38] studied the electrodeposition of Cu–Ni–W incorporated with SiC nanoparticles. They investigated the effects of different concentrations of SiC ranging from 0 to 25 g/L, stir rates ranging from 100 to 600 rpm, and the change in current density from 10 to 50 $mAcm^{-2}$. They optimized the plating conditions to obtain the best wear protection and hardness for the coatings. With the change in concentration from 0 to 25 g/L SiC in the plating solution, 15 g/L was found to have the highest incorporation of SiC into the coating. Also, the 15 g/L incorporation of SiC into the Cu–Ni matrix increased hardness and had the lowest weight loss factor and friction factor from the wear results. It was hypothesized that any amount over 15 g/L caused agglomeration of the SiC particles, which produced observable voids on the surface of the coating in the SEM pictures. A 400 rpm stir rate and the 20 $mAcm^{-2}$ current density proved to be the optimal conditions for the best wear resistance and hardness. The SEM of the coating incorporated with 15 g/L of SiC, stirred at 400 rpm, and electrodepos-

ited with a current density of 20 $mAcm^{-2}$ showed the least amount of visible wear on the surface after testing [38].

Wan et al. [39] developed a continuous three step deposition process to produce Cu, Cu–Fe, and Cu–Ni reinforced carbon fiber (6–8 μm in diameter) composites. Cu–C, Cu–Fe–C, and Cu–Ni–C composites display similar strength vs. temperature graphs to each other, but the decreasing trend seen in the tensile strength is controlled by a different mechanism. A decrease in the tensile strength for the Cu–C composite was due to interfacial bonding at the carbon fiber interface. Interfacial debonding was found to be absent for Cu–Ni–C and Cu–Fe–C composites because its larger interfacial bonding strength is due to a diffusion reaction and a chemical reaction at the interface of the fiber–metal matrix. The maximum tensile strength value was obtained with the addition of Cu–Ni onto the carbon fiber interface, but the optimal tensile strength value was not found to be proportional to the interfacial bonding strength, whereas the highest bonding strength was found for the Cu–Fe–C composite [39].

Our group studied electrodeposited 70–30 Cu–Ni coatings incorporated with a platelet-clay known as montmorillonite (MMT) from a citrate bath. Layered silicates have several advantageous properties to be utilized for composites, such as a high surface area, chemical inertness, resistance to extreme temperatures, and resistance to pH changes. The inclusion of layered silicates, such as MMT, has shown an increase in hardness, adhesion, and corrosion resistance in Ni and Ni–Mo coatings [56–59]. MMT has a 2:1 layered structure, with two layers of the silicon tetrahedral sandwiching one layer of an aluminum octahedral. Seen in Figure 8, MMT is a hydrous aluminum silicate with the formula $(Na,Ca)(Al, Mg)_6(Si_4O_{10})_3\text{-}(OH)_6 \cdot nH2O$ and measures 1 nm in height and 1–2 microns in width [12]. The Al^{3+} and Si^{4+} locations can be replaced by lower valent cations, causing the montmorillonite structure to have an excess of electrons. The negative charge is compensated through loosely held cations from the associated water. Within aqueous solutions, MMT can be completely delaminated and incorporated into other materials, forming continuous, crack-free films, which is a necessary requirement of corrosion resistant coatings [12]. For this work, a solution of MMT was stirred vigorously for 24–48 h to exfoliate the layered silicates. Seen in Table 2, the zeta potential of the plating solution with the dispersed MMT was also evaluated to check the stability of the particles in solution. When dealing with the electrocodeposition of a MMC, understanding the particle stability in the colloidal plating solution is vital because the properties of composites increase significantly with the preferential inclusion of individual particles [2].The exfoliated MMT is stable in solution and easily dispersed into aqueous solutions, while the non-exfoliated MMT precipitates. For stable nanoparticle suspensions, the ideal zeta potential would be a value greater than ±25 mV. The Cu–Ni–MMT plating solutions were around –19 to –20 mV. The adsorption of the Ni and Cu at the surface of the MMT platelet moves the zeta potential toward a more positive value and helps to increase the particle size, which slightly decreases the electrostatic stabilization of the dispersion compared to pure MMT solution. However, the plating solutions still had enough stability for deposition purposes to stay suspended in solution throughout the deposition cycle. Once exfoliated and freely dispersed throughout the electrolytic bath, the MMT platelets can slowly settle down onto the surface of the electrode and be incorporated into the forming alloy coating structure as shown in Figure 1.

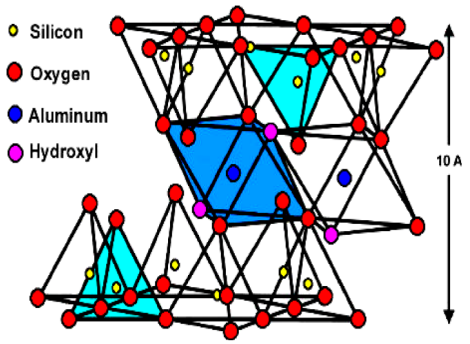


Figure 8. The structure and thickness of montmorillonite [12].

Solutions	Zeta Potential (mV)
0.05% MMT	–38.8
0.1% MMT	–39.2
0.2% MMT	–38.7
Cu–Ni–0.05% MMT	–20.2
Cu–Ni–0.1% MMT	–19.5
Cu–Ni–0.2% MMT	–19.2

Table 2. Zeta potentials for pure MMT and 70–30 Cu–Ni–MMT plating solutions [60].

A copper–nickel alloy (70–30 ratio) was electrochemically deposited from a citrate bath and compared to a composite coating incorporated with 0.05–0.2% MMT to study the effects of the mechanical properties.The adhesion shear strength (Figure 9) and the hardness (Figure 10) for the MMC coatings were investigated. The adhesion shear strength (measured by resistance to knife movement) (Figure 9) was evaluated with MMT amounts in solution ranging from 0 to 0.2% and all of the nanocomposite coatings surpass the strength of the pure Cu–Ni matrix. The shear adhesion tests were measured using the XYZTEC instrument paired with a 2-mm wide knife. The knife was placed at 5 μm above the substrate-coating interface and moved 2 mm horizontally at a velocity 150 (μm/s) through the coatings. With the addition of MMT into the Cu–Ni coating, a greater resistance to the knife movement was observed. The nearly 300% increase from pure Cu–Ni to Cu–Ni–0.05% MMT displays the value that the platelets can have at low loading values.As the MMT in solution increases to 0.1–0.2%, the mechanical resistance of the coating begins to decrease. This indicates that the increased amount of platelets incorporated into the coating leads to more substrate–platelet contact which would reduce the effective area of the matrix–substrate contact and leads to a reduction in the adhesion strength of the coatings. The microhardness test (Figure 10) revealed an increase of about 25% for the Cu–Ni coatings incorporated with MMT versus the pure Cu–Ni coating [60].

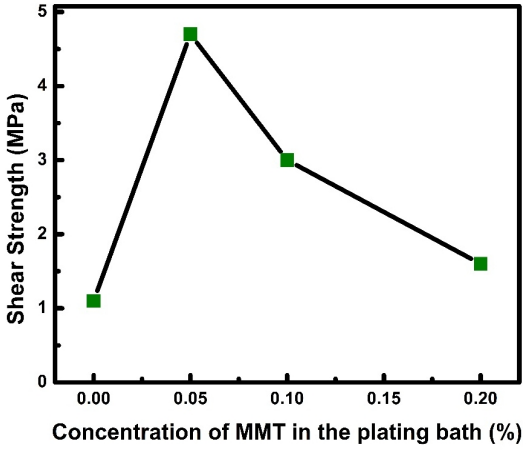


Figure 9. The adhesion shear strength of different coating layers with varying amounts of MMT in the electroplating solution [60].

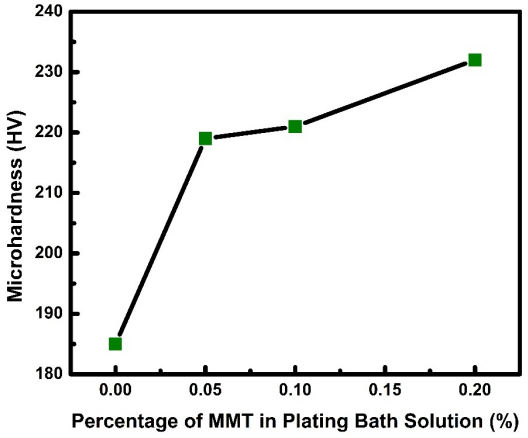


Figure 10. Vickers microhardness for the 70–30 Cu–Ni Coatings incorporated with MMT [60].

4. Cu–Ni MMCs in Electrochemistry and Improved Corrosion Protection

Understanding the relationship between the electrochemical deposition parameters and the resulting corrosion properties is of great importance for creating optimal coatings that will endure harsh environments. MMC coatings that reduce the rate of corrosion at a lower cost have been extensively studied. Exposing films to an unfavorable environment accelerates the

degradation of the coating, which can lead to many different types of corrosion phenomena [61, 62]. The rate of corrosion can be slowed using five universal approaches which include the choice of materials, chemical inhibitors, altercations in the environment, cathodic protection, or coatings [63]. Al particles and MMT were incorporated into the Cu–Ni matrix to understand how magnetic particles affect the metal matrix and MMT to observe how platelets affect the corrosion resistance of the Cu–Ni coating [40, 60].

Cui et al. [40] successfully codeposited Cu–Ni–Al MMCs and noted that high amounts of Al (~3 μm) particles, 29 vol. %, could be deposited into the Cu–Ni coating matrix. They investigated whether the conductive Al particles would behave similar to inert particle codeposition according to the Guglielmi's model. Adding the conductive aluminum particles into the Cu–Ni matrix caused the polarization curve to shift to more negative potentials, which was credited to the non-active surface of the aluminum metal particles during the deposition of Cu–Ni following a similar codeposition path for inert particles defined by Guglielmi. The parameters used in Guglielmi's model for the codeposition of non-conductive inert particles can also model the deposition of charged particles presented in this research [40].

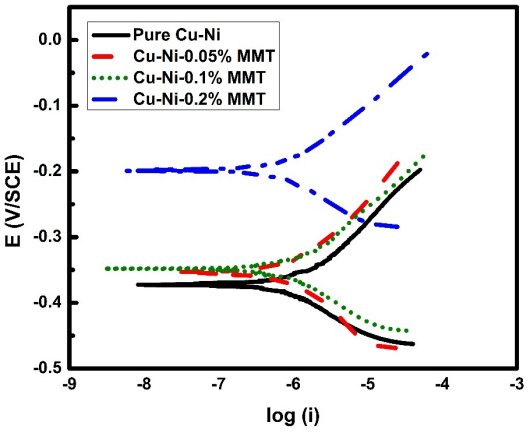


Figure 11. Tafel plots for the 70–30 Cu–Ni coatings with and without MMT after being submerged in a 3.5 % NaCl solution for two weeks [60].

In addition to the mechanical properties, our group studied the corrosion behaviors of the 70–30 Cu–Ni–MMT coatings by the use of Tafel polarization and electrochemical impedance spectroscopy (EIS). The corrosion of 70–30 Cu–Ni and 70–30 Cu–Ni–MMT composite coatings were evaluated using potentiodynamic polarization, as seen in Figure 11. The corrosion parameters were measured after immersing the 70–30 Cu–Ni coatings for two weeks in 3.5% NaCl solution at 25°C. The E_{corr} and I_{corr} correlation for the Cu–Ni–MMT coatings can be seen in Figure 12. Figure 12 shows E_{corr} shifting to more positive potentials and the I_{corr} shifting to lower current values leading to the Cu–Ni–0.2% MMT having the best corrosion properties. Nyquist plots (Figure 13) of pure Cu–Ni and Cu–Ni–0.2% MMT composite coatings after 14 days immersion in 3.5 % NaCl at 25°C showed the diameter of the depressed uncompleted

semicircles is larger in case of Cu–Ni–MMT compared to pure Cu–Ni, which displays increased stability of the passive film in the case of Cu–Ni–MMT compared to that of pure Cu–Ni coating. The equivalent circuit parameters of the fitting procedure showed an increase in R_p from 2.87 kΩcm^2 (pure Cu–Ni) to 13.77 kΩcm^2 (Cu–Ni–0.2% MMT), as seen in Table 3. The calculated parameters show higher resistance for the inner layer in case of Cu–Ni–MMT composite coating compared to that of pure Cu–Ni; this resistance increases as the MMT content in the metallic matrix increases, which is consistent with the data obtained from potentiodynamic polarization, and also confirms that embedding of layered silicate particles into the Cu–Ni metallic matrix increases its corrosion resistance [60].

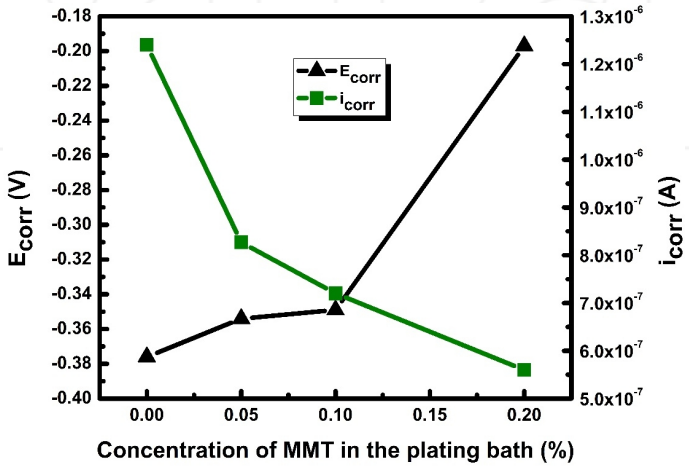


Figure 12. E_{corr} and i_{corr} of 70–30 Cu–Ni coatings incorporated with MMT [60].

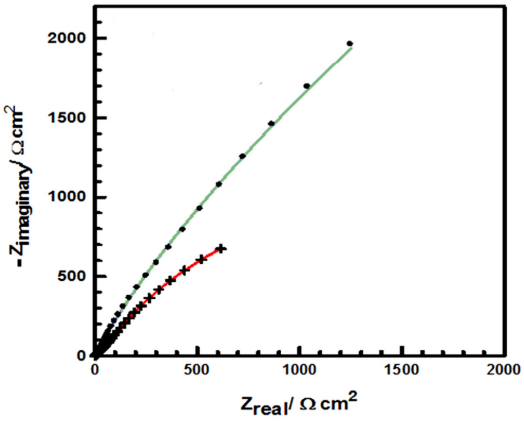


Figure 13. Nyquist impedance plots of pure Cu–Ni (A) and Cu–Ni–0.2% MMT (B) after being submerged in a 3.5% NaCl solution for two weeks [60].

Coatings	R_s (Ω cm^2)	R_1 (Ω cm^2)	Q_1 (Ω^{-1} s$^{\alpha}$ cm^{-2})	α_1	R_p (kΩ cm^2)	Q_2 (Ω^{-1} s$^{\alpha}$ cm^{-2})	α_2
Cu–Ni	2.25	49.78	2.95×10^{-3}	0.56	2.87	1336×10^{-6}	0.73
Cu–Ni–0.05% MMT	0.78	5.45	6.20×10^{-3}	0.75	3.02	954×10^{-6}	0.75
Cu–Ni–0.1% MMT	5.01	54.0	1.26×10^{-3}	0.68	4.92	709×10^{-6}	0.80
Cu–Ni–0.2% MMT	8.32	95.20	2.33×10^{-6}	0.99	13.77	583×10^{-6}	0.76

Table 3. The equivalent circuit parameters of Cu–Ni and Cu–Ni–MMT composite coatings after two weeks submersion in a 3.5% NaCl solution [60].

5. Conclusions

Electrodeposition provides a versatile and convenient route for controlled coating of composites (i.e. materials having more than one phase) containing nano- to microparticles dispersed in a metal matrix for material science and engineering applications. Enhancement of the electrical, mechanical, and corrosion properties of the coatings is observed with the inclusion of different particles into the Cu–Ni matrix. With the increase in availability of micro- and nanoparticles, more research needs to be performed in the area of Cu–Ni MMCs to further explore their beneficial properties.

Acknowledgements

This work was made possible by NPRP Grant 4-306-2-111 from the Qatar National Research Fund (a Member of the Qatar Foundation). The statements made herein are solely the responsibility of the authors. The authors would also like to thank Jonathan Bishop for help with the figures.

Author details

Casey R. Thurber[1], Adel M.A. Mohamed[2,3*] and Teresa D. Golden[1]

*Address all correspondence to: adel.mohamed25@yahoo.com

1 Department of Chemistry, University of North Texas, Denton, Texas, USA

2 Department of Metallurgical and Materials Engineering, Faculty of Petroleum and Mining Engineering, Suez University, Egypt

3 Center for Advanced Materials, Qatar University, Doha, Qatar

References

[1] Musiani M. Electrodeposition of composites: an expanding subject in electrochemical materials science. Electrochim. Acta. 2000;45:3397–3402. DOI: 10.1016/S0013-4686(00)00438-2.

[2] Gomes A, Pereira I, Fernández B, Pereiro R. Electrodeposition of metal matrix nanocomposites: Improvement of the chemical characterization techniques. Advances in Nanocomposites - Synthesis, Characterization and Industrial Applications. Intech. 2011;21:503-526. DOI: 10.5772/15557.

[3] Walsh FC, Ponce de Leon C. A review of the electrodeposition of metal matrix composite coatings by inclusion of particles in a metal layer: an established and diversifying technology. Trans. Inst. Met. Finish. 2014;92:83-98. DOI: 10.1179/0020296713Z.000000000161.

[4] Hovestad A, Jansen LJJ. Electrochemical codeposition of inert particles in a metallic matrix. J. Appl. Electrochem. 1995;25:519-527. DOI 10.1007/BF00573209.

[5] Panda A, Podlaha EJ, Nanoparticles to improve mass transport inside deep recesses. Electrochem. Solid St., 2003;6:C149-C152. DOI: 10.1149/1.1614452.

[6] Chen YC, Liu W, Chao T, Cheng YT. An optimized Cu-Ni nanocomposite coil for low-power electromagnetic microspeaker fabrication. Transducers. 2009:25-28. DOI: 10.1109/SENSOR.2009.5285572.

[7] Chiriac H, Moga AE, Constantin VA. Synthesis and magnetic properties of Fe-Ni and Cu-Ni composite coatings. J. Optoelectron Adv. M. 2007;9:1161-1164.

[8] Huang Z, Peng X, Wang F. Preparation and oxidation of novel electrodeposited Cu–Ni–Cr nanocomposites. Oxid. Met. 2006;65:223-235. DOI: 10.1007/s11085-006-9017-y.

[9] Huang Z, Peng X, Xu C, Wang F. On the exclusive growth of external chromia scale on the novel electrodeposited Cu–Ni–Cr nanocomposites. J. Mater. Res. 2007;22:3166-3177. DOI: 10.1557/JMR.2007.0411.

[10] Huang YW, Chao T, Chen CC, Cheng YT. Power consumption reduction scheme of magnetic microactuation using electroplated Cu–Ni nanocomposite. App. Phys. Letters. 2007;90:1-3. DOI: 10.1063/1.2748301.

[11] Bard AJ, Faulkner LR. Electrochemical Methods: Fundamentals and Applications. New York, 2000. ISBN: 0-471-04372-9.

[12] Horch RA, Golden TD, D' Souza NA, Riester L. Electrodeposition of nickel/montmorillonite layered silicate nanocomposite thin films. Chem. Mater. 2002;14:3531-3538. DOI: 10.1021/cm010812+.

[13] Harrigan WC. Commercial processing of metal matrix composites. Mater. Sci. Eng. 1998;A244:75–79. DOI: 10.1016/S0921-5093(97)00828-9.

[14] Zeng X, Tao Z, Zhu B, Zhou E, Cui K. Investigation of laser cladding ceramic-metal composite coatings: processing modes and mechanisms. Surf. Coat. Tech. 1996;79:209-217. DOI: 10.1016/0257-8972(95)02431-X.

[15] Lindroos VK, Talvitie MJ. Recent advances in metal matrix composites. J. Mater. Process. Tech. 1995;53:273-284. DOI: 10.1016/0924-0136(95)01985-N.

[16] Deuis RL, Yellup JM, Subramanian C. Metal-matrix composite coatings by PTA surfacing. Compos. Sci. Technol. 1998;58:299-309. DOI: 10.1016/S0266-3538(97)00131-0.

[17] Hashim J, Looney L, Hashmi MSJ. Metal matrix composites: production by the stir casting method. J. Mater. Process. Tech. 1999;92-93:1-7. DOI: 10.1016/S0924-0136(99)00118-1.

[18] Muratoglu M, Yilmaz O, Aksoy M. Investigation on diffusion bonding characteristics of aluminum metal matrix composites (Al/SiCp) with pure aluminum for different heat treatments. J. Mater. Process. Tech. 2006;178:211–217. DOI: 10.1016/j.jmatprotec.2006.03.168.

[19] Tan MJ, Zhang X. Powder metal matrix composites: selection and processing. Mater. Sci. Eng. 1998;A244:80–85. DOI: 10.1016/S0921-5093(97)00829-0.

[20] Popovskaa N, Gerhard H, Wurm D, Poscher S, Emig G, Singer RF. Chemical vapor deposition of titanium nitride on carbon fibers as a protective layer in metal matrix composites. Mater. Design. 1997;18:239-242. DOI: S0261–3069(97)00057–5.

[21] Chrobak A, Kubisztal M, Kubisztal J, Chrobak E, Haneczok G. Microstructure, magnetic and elastic properties of electrodeposited Cu+Ni nanocomposites coatings. J. Achieve. Mater. Manufac. Eng. 2011;49:17-26.

[22] Rosso M. Ceramic and metal matrix composites: Routes and properties. J. Mater. Process. Tech. 2006;175:364–375. DOI: 10.1016/j.jmatprotec.2005.04.038.

[23] Pradhan AK, Das S. Pulse-reverse electrodeposition of Cu–SiC nanocomposite coating: Effect of concentration of SiC in the electrolyte. J. Alloy Compd. 2014;590:294–302. DOI: 10.1016/j.jallcom.2013.12.139.

[24] Zamblau I, Varvara S, Muresan LM. Corrosion behavior of Cu–SiO_2 nanocomposite coatings obtained by electrodeposition in the presence of cetyl trimethyl ammonium bromide. J. Mater. Sci. 2011;46:6484–6490. DOI: 10.1007/s10853-011-5594-5.

[25] Ramalingam S, Muralidharan VS, Subramania A. Electrodeposition and characterization of Cu-TiO_2 nanocomposite coatings. J. Solid State Electrochem. 2009;13:1777–1783. DOI: 10.1007/s10008-009-0870-x.

[26] Gan Y, Lee D, Chen X, Kysar JW. Structure and properties of electrocodeposited Cu–Al_2O_3 nanocomposite thin films. J. Mater. Process. Tech. 2005;127:451-456. DOI: 10.1115/1.1925292.

[27] Mangam V, Bhattacharya S, Das K, Das S. Friction and wear behavior of Cu–CeO_2 nanocomposite coatings synthesized by pulsed electrodeposition. Surf. Coat. Tech. 2010;205:801–805. DOI: 10.1016/j.surfcoat.2010.07.119.

[28] Rusu DE, Cojocaru P, Magagnin L, Gheorghies C, Carac G. Study of Ni-TiO_2 nanocomposite coating prepared by electrochemical deposition. J. Optoelectron Adv. M. 2010;12:2419-2422.

[29] Sen R, Das S, Das K. Synthesis and properties of pulse electrodeposited Ni-CeO_2 nanocomposite. Metall. Mater. Trans. A. 2012;43A:3809-3823. DOI: 10.1007/s11661-012-1170-0.

[30] Vaezi MR, Sadrnezhaad SK, Nikzad L. Electrodeposition of Ni–SiC nano-composite coatings and evaluation of wear and corrosion resistance and electroplating characteristics. Colloids and Surf. A. 2008;315:176-182. DOI: 10.1016/j.colsurfa.2007.07.027.

[31] Chang LM, Liu JH, Zhang RJ. Corrosion behaviour of electrodeposited Ni/Al_2O_3 composite coating covered with a NaCl salt film at 800 °C. Mater. Corros. 2011;62:920-925. DOI: 10.1002/maco.200905617.

[32] Kasturibai S, Kalaignan GP. Physical and electrochemical characterizations of Ni-SiO_2 nanocomposite coatings. Ionics. 2012:1-8. DOI 10.1007/s11581-012-0810-0.

[33] Conrad HA, Corbett JR, Golden TD. Electrochemical deposition of γ-phase zinc-nickel alloys from alkaline solution. J. Electrochem. Soc. 2012;159:C29-C32. DOI: 10.1149/2.027201jes.

[34] Ahmad YH, Mohamed AMA, Golden TD, D'Souza N. Electrodeposition of nanocrystalline Ni-Mo alloys from alkaline glycinate solutions. Int. J. Electrochem. Sci. 2014;9:6438-6450.

[35] Yuan SJ, Pehkonen SO. Surface characterization and corrosion behavior of 70/30 Cu–Ni alloy in pristine and sulfide-containing simulated seawater. Corros. Sci. 2007;49:1276-1304. DOI: 10.1016/j.corsci.2006.07.003.

[36] Low CTJ, Wills RGA, Walsh FC. Electrodeposition of composite coatings containing nanoparticles in a metal deposit. Surf. Coat. Tech. 2006;201:371–383. DOI:10.1016/j.surfcoat.2005.11.123.

[37] Fawzy MH, Ashour MM, El-Halim ABD. Effect of some operating variables on the characteristics of electrodeposited Cu-Ni alloys with and without α-$A1_2O_3$ and TiO_2 inert particles. J. Chem. Tech. Biotechnol. 1996;66:121-130. DOI: 10.1002/(SICI)1097-4660(199606)66:2<121::AID-JCTB475>3.0.CO;2-A.

[38] Hashemi M, Mirdamadi SH, Rezaie HR. Effect of SiC nanoparticles on microstructure and wear behavior of Cu-Ni-W nanocrystalline coating. Electrochim. Acta. 2014;138:224–231. DOI: 10.1016/j.electacta.2014.06.084.

[39] Wan YZ, Wang YL, Luo HL, Dong XH, Cheng GX. Effects of fiber volume fraction, hot pressing parameters and alloying elements on tensile strength of carbon fiber reinforced copper matrix composite prepared by continuous three-step electrodeposition. Mater. Sci. Eng. 2000;A288:26–33. DOI: S0921-5093(00)00887-X.

[40] Cui X, Wei W, Liu H, Chen W. Electrochemical study of codeposition of Al particle—Nanocrystalline Ni/Cu composite coatings. Electrochim. Acta. 2008;54:415–420. DOI: 10.1016/j.electacta.2008.07.066.

[41] Mohan S, Rajasekaren N. Influence of electrolyte pH on composition, corrosion properties and surface morphology of electrodeposited Cu-Ni alloy. Surf. Eng. 2011;7:519-523. DOI: 10.1179/026708410X12786785573472.

[42] Green TA, Russell AE, Roy SJ. The development of a stable citrate electrolyte for the electrodeposition of copper-nickel alloys. J. Electrochem. Soc. 1998;145:875-881. DOI: 10.1149/1.1838360.

[43] Varea A, Pellicer E, Pané S, Nelson BJ, Suriñach S, Baró MD, Sort J. Mechanical properties and corrosion behavior of nanostructured Cu-rich CuNi electrodeposited films. Int. J. Electrochem. Sci. 2012;7:1288-1302.

[44] Rode S, Henninot C, Vallières C, Matlosz M. Complexation chemistry in copper plating from citrate baths. J. Electrochem. Soc. 2004;151:C405-C411. DOI: 10.1149/1.1869980.

[45] Orniakova R, Turonova A, Kladekova D, Galova M, Smith RM. Recent developments in the electrodeposition of nickel and some nickel-based alloys. J. Appl. Electrochem. 2006;36:957–972. DOI: 10.1007/s10800-006-9162-7.

[46] Alper M, Kockar H, Safak M, Baykul MC. Comparison of Ni-Cu alloy films electrodeposited at low and high pH levels. J. Alloys Compd. 2008;453:15-19. DOI: 10.1016/j.jallcom.2006.11.066.

[47] Metikos-Hukovic M, Skugor I, Grubac Z, Babic R. Complexities of corrosion behaviour of copper–nickel alloys under liquid impingement conditions in saline water. Electrochim. Acta. 2010;55:3123-3129. DOI: 10.1016/j.electacta.2010.01.066.

[48] Boyapati VAR, Kanukula CK. Corrosion inhibition of Cu-Ni (90/10) alloy in seawater and sulphide-polluted seawater environments by 1, 2, 3-Benzotriazole. ISRN Corros. 2013;2013:1-22. DOI: 10.1155/2013/703929.

[49] Bautista BET, Carvalho ML, Seyeux A, Zanna S, Cristiani P, Tribollet B, Marcus P, Frateur I. Effect of protein adsorption on the corrosion behavior of 70Cu-30Ni alloy in artificial seawater. Bioelectroch. 2014;97:34-42. DOI: 10.1016/j.bioelechem.2013.10.004.

[50] Milosev I, Metikos-Hukovic M. The behaviour of Cu-xNi (x = 10 to 40 wt%) alloys in alkaline solutions containing chloride ions. Electrochim. Acta. 1997;42:1537-1548. DOI: S0013-4686(96)00315.

[51] Williams RV, Martin PW. Electrodeposited composite coatings. Trans. Inst. Met. Finish. 1964;42:182-187.

[52] Brandes EA, Goldthorpe D. Co-deposition of metals and ceramic particles. Metallurgia. 1967;76:195–198.

[53] Guglielm N. Kinetics of the deposition of inert particles from electrolytic baths. J. Electrochem. Soc. 1972;119:1009-1012. DOI: 10.1149/1.2404383.

[54] Celis JP, Roos JR, Buelens C. A mathematical model for the electrolytic codeposition of particles with a metallic matrix. J. Electrochem. Soc. 1987;134:1402–1408. DOI: 10.1149/1.2100680.

[55] Bercot P, Pena-Munoz E, Pagetti J. Electrolytic composite Ni PTFE coatings: An adaptation of Guglielmi's model of the phenomena of incorporation. Surf. Coat. Technol. 2002;157:282–289. DOI: S0257-8972Ž02.00180-9.

[56] Tientong J, Thurber CR, D'Souza N, Mohamed AMA, Golden TD. Influence of bath composition at acidic pH on electrodeposition of nickel-layered silicate nanocomposites for corrosion protection. Int. J. Electrochem. 2013;2013:1-8. DOI: 10.1155/2013/853869.

[57] Tientong J, Ahmad YH, Nar M, D'Souza N, Mohamed AMA, Golden TD. Improved mechanical and corrosion properties of nickel composite coatings by incorporation of layered silicates. Mater. Chem. Phys. 2014;145:44-50. DOI: 10.1016/j.matchemphys.2014.01.025.

[58] Ahmad YH, Tientong J, D'Souza N, Golden TD, Mohamed AMA. Salt water corrosion resistance of electrodeposited Ni-layered silicate nanocomposite coatings from Watts' Type Solution. Surf. Coat. Tech. 2014;242:170-176. DOI: 10.1016/j.surfcoat.2014.01.040.

[59] Thurber CR, Calhoun MC, Ahmad YH, D'Souza N, Mohamed AMA, Golden TD, Electrodeposition of Cu-Ni incorporated with layered silicates for corrosion protection. ECS Trans. 2014;61:49-60. DOI: 10.1149/06120.0049ecst.

[60] Thurber CR, Ahmad YH, Sanders SF, Al-Shenawa A, D'Souza N, Mohamed AMA, Golden TD. Electrodeposition of 70-30 Cu-Ni nanocomposite coatings for enhanced mechanical and corrosion properties. Curr. Appl. Phys. 2016;16:387-396. DOI: 10.1016/j.cap.2015.12.022.

[61] Chang YY, Wang DY. Corrosion behavior of electroless nickel-coated AISI 304 stainless steel enhanced by titanium ion implantation. Surf. Coat. Tech. 2005;200:2187-2191. DOI: 10.1016/j.surfcoat.2004.07.118.

[62] Tang PT, Pulse reversal plating of nickel alloys. Institute of Metal Finishings. 2007;85:51-56. DOI: 10.1179/174591907X162459.

[63] Painting: New Construction and Maintenance, U.S Army Corps of Engineers EM 1110-2-3400, 2-1 1995.

INTECH